JOURNAL OF THE AMERICAN CHEMICAL SOCIETY

University of Texas Libraries

Subscriber access provided by University of Texas Libraries

Communication

Design and Remarkable Efficiency of the Robust Sandwich Cluster Composite Nanocatalysts ZIF-8@Au25@ZIF-67

Yapei Yun, Hongting Sheng, Kang Bao, Li Xu, Yu Zhang, Didier Astruc, and Manzhou Zhu

J. Am. Chem. Soc., **Just Accepted Manuscript** • DOI: 10.1021/jacs.0c00378 • Publication Date (Web): 12 Feb 2020

Downloaded from pubs.acs.org on February 14, 2020

Just Accepted

"Just Accepted" manuscripts have been peer-reviewed and accepted for publication. They are posted online prior to technical editing, formatting for publication and author proofing. The American Chemical Society provides "Just Accepted" as a service to the research community to expedite the dissemination of scientific material as soon as possible after acceptance. "Just Accepted" manuscripts appear in full in PDF format accompanied by an HTML abstract. "Just Accepted" manuscripts have been fully peer reviewed, but should not be considered the official version of record. They are citable by the Digital Object Identifier (DOI®). "Just Accepted" is an optional service offered to authors. Therefore, the "Just Accepted" Web site may not include all articles that will be published in the journal. After a manuscript is technically edited and formatted, it will be removed from the "Just Accepted" Web site and published as an ASAP article. Note that technical editing may introduce minor changes to the manuscript text and/or graphics which could affect content, and all legal disclaimers and ethical guidelines that apply to the journal pertain. ACS cannot be held responsible for errors or consequences arising from the use of information contained in these "Just Accepted" manuscripts.

is published by the American Chemical Society. 1155 Sixteenth Street N.W., Washington, DC 20036

Published by American Chemical Society. Copyright © American Chemical Society. However, no copyright claim is made to original U.S. Government works, or works produced by employees of any Commonwealth realm Crown government in the course of their duties.

Design and Remarkable Efficiency of the Robust Sandwich Cluster Composite Nanocatalysts ZIF-8@Au$_{25}$@ZIF-67

Yapei Yun,[†§] Hongting Sheng,*[,†§] Kang Bao,[†§] Li Xu,[†§] Yu Zhang,[†§] Didier Astruc,*[,‡] Manzhou Zhu*[,†§]

† Department of Chemistry and Center for Atomic Engineering of Advanced Materials, Anhui Province Key Laboratory of Chemistry for Inorganic/Organic Hybrid Functionalized Materials, Anhui University, Hefei, Anhui 230601, China

§ Key Laboratory of Structure and Functional Regulation of Hybrid Materials (Anhui University), Ministry of Education, Hefei 230601, China

‡ Université de Bordeaux, ISM, UMR CNRS N° 5255, 351 Cours de la Libération, 33405 Talence Cedex, France

Supporting Information Placeholder

ABSTRACT: Heterogeneous catalysts with precise surface and interface structures are of great interest to decipher the structure–property relationships and maintain remarkable stability while achieving high activity. Here, we report the design and fabrication of the new sandwich composites ZIF-8@Au$_{25}$@ZIF-67[tkn] and ZIF-8@Au$_{25}$@ZIF-8[tkn] [tkn = thickness of shell] by coordination-assisted self-assembly with well-defined structures and interfaces. The composites ZIF-8@Au$_{25}$@ZIF-67 efficiently catalyzed both 4-nitrophenol reduction and terminal alkyne carboxylation with CO_2 under ambient conditions with remarkably improved activity and stability, compared to the simple components Au$_{25}$/ZIF-8 and Au$_{25}$@ZIF-8, highlighting the highly useful function of the ultrathin shell. In addition, the performances of these composite sandwich catalysts are conveniently regulated by the shell thickness. This concept and achievements should open a new avenue to the targeted design of well-defined nanocatalysts with enhanced activities and stabilities for challenging reactions.

With the ever-increasing desire toward sustainable energy, a great deal of efforts have been devoted to the design of heterogeneous nanocatalysts.[1] In some cases, special emphasis is placed on improving reactivity of these nanomaterials while ignoring their stability.[2] In fact, the stability of heterogeneous nanocatalysts, especially for ultrasmall metal nanoparticles, is a key parameter for practical utilizations and should be one of the most sought properties, because stability guarantees catalytic recyclability.[3] Various strategies have been developed to pursue nanocatalysts with remarkable activity and stability,[4] among which the combination of MNPs (metal nanoparticles) and MOFs (metal-organic frameworks) holds great promise.[5] Indeed MNP-decorated MOF nanocomposites are endowed with additional active sites to work synergistically, and confined effects prevent MNP aggregation, resulting in a well enhanced catalytic performance.

Recently, a growing number of publications have indicated that the catalytic performance of MNP-decorated MOF nanocomposites markedly depends on the MNP location relative to the MOF.[6] In most cases, MNPs/MOFs (MNPs deposited on the surface of MOFs) exhibit high activity but low stability, because MNPs loaded on the outer surface easily fall off. On the other hand MNPs@MOFs (MNPs intercalated in MOFs) present a good stability but poor activity owing to high diffusion resistance that hinders the access of reactants to the MNPs.[6b-d] Therefore, this creates a dilemma regarding the expected target for an ideal MNP-decorated MOF nanocomposite with enhanced reactivity and excellent stability for a given reaction. Sandwich MOFs@MNPs @MOFs composites may be able to work to this end, because the sandwich structure maximizes the metal-support interface to regulate the activity, and the controllable shell prevents MNPs from separating during the reaction process. Tang's group fabricated sandwich MIL-101@Pt@MIL-101 composite exhibiting a considerable improvement in the reactivity, stability and selectivity for the hydrogenation of α,β-unsaturated aldehydes compared with the corresponding Pt@MIL-101.[7] Despite this success for MOFs@MNPs@MOFs, the key drawback herein is the ill-defined MNPs and blurred interaction at the interfaces (the inevitable presence of a stabilizing polymer (PVP) in the obtained MOFs@MNPs@MOFs) that impedes the clarification of the structure–property relationships. To our knowledge, an effective and general solution to overcome this challenge has not yet appeared. In light of these requirements, we inferred that the catalysts MOFs@APNCs@MOFs (APNCs: monodisperse atomically precise nanoclusters), in which all the components are well-defined, would work to this end, i.e., allow to better decipher the structure–property relationships at the molecular level.[4c, 8] Moreover, the comparison of the catalytic properties of three monodisperse APNCs-decorated MOF nanomaterials: APNCs/MOFs, APNCs@MOFs and MOFs@APNCs@MOFs would be conducive to draw a rigorous conclusion toward precise customization of

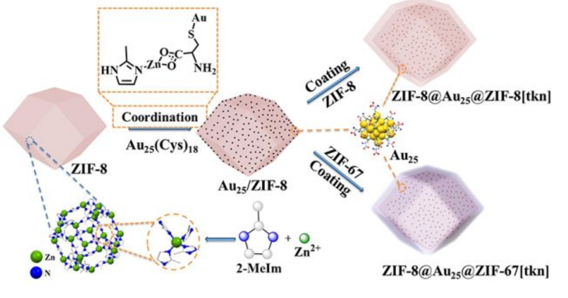

Scheme 1. Synthetic route for the sandwich structures of ZIF-8@Au$_{25}$@ZIF-67[tkn] and ZIF-8@Au$_{25}$@ZIF-8[tkn] [tkn = thickness of shell].

APNCs-decorated MOF nanocatalysts. Our strategy for fabricating the sandwich nanomaterial MOF@APNCs@MOF involved a design by coordination-assisted self-assembly including a three-step process (Scheme 1). First, the nanocluster $Au_{25}(Cys)_{18}$ [9] with terminal ligand groups COOH and ZIF-8[10] were synthesized, characterized by TEM and UV-vis. spectroscopy (Figure S1), and evenly dispersed in aqueous solution, respectively. Then a solution of $Au_{25}(Cys)_{18}$ was slowly poured into the ZIF-8 solution via physical impregnation to form the nanomaterial Au_{25}/ZIF-8 that was characterized by TEM (Figure S2) and IR spectroscopy (Figure 1B). Finally, the composite Au_{25}/ZIF-8 was further uniformly dispersed in methanol solution, and the solution of $Co(NO_3)_2$ at a specific concentration was slowly added to the solution of Au_{25}/ZIF-8, resulting in Co^{2+} coating on the Au_{25}/ZIF-8 surface by coordination between Co^{2+} and the carboxylate group. The solution of 2-MeIm was slowly added to the above system, and the sandwich composite ZIF-8@Au_{25}@ZIF-67 was obtained by gentle agitation at room temperature for 24 hours. To the best of our knowledge, this is the first report on the rational fabrication of APNCs-decorated MOF sandwich materials. Interestingly, the shell thickness of ZIF-8@Au_{25}@ZIF-67[tkn] was controlled at will by precisely adjusting the concentration of 2-MeImA and Co^{2+} solution. In addition, the nanomaterials ZIF-8@Au_{25}@ZIF-8[tkn] were also fabricated using the same strategy.

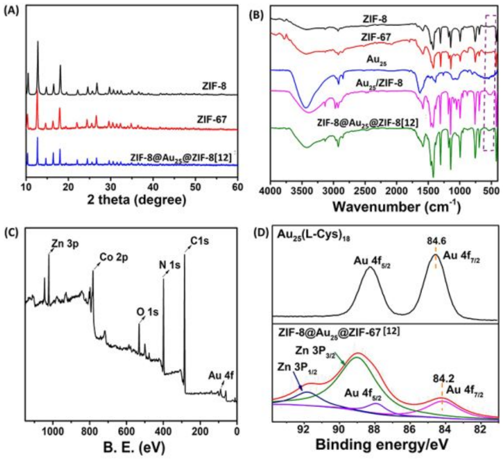

Figure 1. (A) XRD patterns of ZIF-8, ZIF-67 and ZIF-8@Au_{25}@ZIF-67[12]; (B) FTIR characterization of ZIF-8, ZIF-67, Au_{25}/ZIF-8 and ZIF-8@Au_{25}@ZIF-67[12]; (C) XPS spectrum of ZIF-8@Au_{25}@ZIF-67[12]; (D) XPS spectrum of Au in $Au_{25}(Cys)_{18}$ and ZIF-8@Au_{25}@ZIF-67[12].

The composite nanomaterial ZIF-8@Au_{25}@ZIF-67[12] was characterized by X-ray diffraction (XRD), Fourier-transform infrared (FT-IR), X-ray photoelectron spectroscopy (XPS) analysis, and N_2 absorption-desorption isothermal (BET). The XRD pattern of ZIF-8@Au_{25}@ZIF-67[12] revealed that there was no significant crystallinity loss after embedding Au_{25} into the ZIF interlayer, indicating that the addition of Au_{25} did not affect the ZIF skeleton (Figure 1A). There is no peak of Au in the XRD pattern, indicating that the size of Au_{25} NC is ultra-small. The coordination interaction between COO^- in Au_{25} NC ligand and Zn^{2+} or Co^{2+} ions was detected by Fourier transform infrared spectroscopy (FT-IR). From Figure 1B, ZIF-8@Au_{25}@ZIF-67[12] shows a new peak at 520 cm^{-1}, which is attributed to the Zn-O (or Co-O) stretching vibration,[11] indicating that Au-Cys-Co or Au-Cys-Zn linkage is the key for self-assembling. XPS analysis confirmed the existence of Au_{25} NC, ZIF-8, and ZIF-67 in the ZIF-8@Au_{25}@ZIF-67[12] composite. The XPS result revealed the presence of Au, S, Co, Zn, and N in the composite (Figure 1C). As shown in Figure 1D, the Au $4f_{7/2}$ of ZIF-8@Au_{25}@ZIF-67[12] (84.2 eV) exhibits a slight negative shift compared to $Au_{25}(Cys)_{18}$ (84.6 eV) likely due to the electron transfer between $Au_{25}(Cys)_{18}$ and ZIF-8 or ZIF-67. This is consistent with the interaction between $Au_{25}(SG)_{18}$ (83.7 eV) and $Au_{25}(SG)_{18}$/ZIF-8 (84.1 eV).[9,12] BET shows ZIF-8@Au_{25}@ZIF-67[12] has similar isothermal features (Figure S3) and a pore diameter ~1.1 nm (Table S1) to ZIF-8 and ZIF-67, indicating that the porous structures of the ZIF-67 and ZIF-8 matrices remain intact after embedding $Au_{25}(Cys)_{18}$. The surface area of ZIF-8@Au_{25}@ZIF-67[12] increased correspondingly, which is presumably related to the self-assembly (Table S1). The morphology and composition of ZIF-8@Au_{25}@ZIF-67[12] were characterized by TEM and energy dispersive X-ray spectroscopy (EDS) (Figure 2).

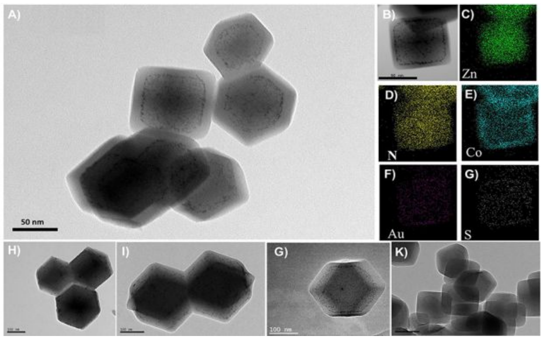

Figure 2. TEM images of (A) ZIF-8@Au_{25}@ZIF-67[12], (B-G) High-angle annular dark field scanning transmission electron microscopy (HAADF-STEM) images and corresponding EDS elemental (C, N, Zn, Co, Au, S) mapping of ZIF-8@Au_{25}@ZIF-67[12]; (H) ZIF-8@Au_{25}@ZIF-67[2], (I) ZIF-8@Au_{25}@ZIF-67[8], (J) ZIF-8@Au_{25}@ZIF-67[18], and (K) ZIF-8@Au_{25}@ZIF-67[25].

The nanocomposite presents a sandwich-like structure with a shell of about 12 nm (Figure 2A). It also clearly appears that the nanoclusters Au_{25} NCs are evenly distributed in the interlayer of the ZIF-8@Au_{25}@ZIF-67[12] in the TEM micrograph. The composition and element distribution of ZIF-8@Au_{25}@ZIF-67[12] further confirm that the surface of Au_{25}/ZIF-8 is fully covered by the ZIF-67 shell (Figure 2B-G). The ZIF-8@Au_{25}@ZIF-67[2], ZIF-8@Au_{25}@ZIF-67[8], ZIF-8@Au_{25}@ZIF-67[18] and ZIF-8@Au_{25}@ZIF-67[25] with different shell thicknesses were successfully prepared by regulation of the concentration of Co^{2+} and characterized by TEM (Figure 2H-K) and EDS energy spectrum element diagrams, respectively (Figure S4-S6, S8). In the meantime, the Au_{25} NCs did not aggregate in these nanomaterials, and most of their sizes were less than 1.2 nm (Figure 2A-K). The EDS line scanning of ZIF-8@Au_{25}@ZIF-67[18] verifies the shell thickness (Figure S7), consistent with the TEM results. Using the same strategy, ZIF-8@Au_{25}@ZIF-8[12] was successfully synthesized by replacing $Co(NO_3)_2$ by $Zn(NO_3)_2$, and related characterizations were performed (Figure S9). All the above results indicate that the "coordination-assisted self-assembly" strategy for the fabrication of MOFs@APNCs@MOFs is effective and universal. It guarantees the integrity of the Au_{25} NCs. Importantly this method avoids the use of PVP and ensures the atomic accuracy of the whole structure.

The useful carboxylation using CO_2 of terminal alkyne was selected as a model reaction to explore the influence of the fixation location of Au_{25} NC on the catalytic performance and to compare with Au_{25}/ZIF-8 and Au_{25}@ZIF-8 [12] (Figure 3). As shown in Figure 3A, the superior performance of ZIF-8@Au_{25}@ZIF-67[12], i.e. remarkable maintenance of 99% yield even after 3 cycles (Figure 3B), is evidently better than that of all the other catalysts, including Au_{25}/ZIF-8 (40.5%) and Au_{25}@ZIF-8 (38.2%), Au_{25} NC (10.8%), ZIF-8 (27.9%) and ZIF-8@ZIF-67 (52.3%). ZIF-8@Au_{25}@ZIF-67[12] is one of the rare examples in which the Au catalyst exhibits high performance for the carboxylation reactions of alkynes under mild conditions (The TON value reached 4433, Table S2). By contrast, the activity of Au_{25}/ZIF-8 decreased significantly after the first cycle. In addition, the reactivity of Au_{25}@ZIF-8 is as low as hypothesized. Then, ZIF-8@Au_{25}@ZIF-67 composites with different shell thicknesses were tested (Figure 3C). Interestingly, the shell thickness had a significant effect on the activity. At the beginning, the activity increased with the thickness. The highest activity occurred for a thickness of 12 nm. Starting at 12 nm, the activity began to decline slowly as the shell thickness increased. This suggests that the shell may have other beneficial effects on the reaction beyond the mass transfer and the stability of the material. We then used temperature-programmed desorption (TPD) of CO_2 to confirm that the shell does help capture and activate the CO_2 molecules (Figure 3D).[13] At the same time, the high activity of ZIF-8@Au_{25}@ZIF-67[12] (99%) compared to that of ZIF-8@Au_{25}@ZIF-8[12] (69%) also highlights the fact that the ZIF-67 shell is responsible for the enhancement of the catalytic performance of ZIF-8@Au_{25}@ZIF-67 (Figure 3A). All these results confirmed that the catalytic performance of sandwich systems is precisely optimized by controlling the shell thickness. To further confirm the excellent stability of the sandwich nanomaterial, we characterized the used ZIF-8@Au_{25}@ZIF-67[12] after five cycles and compared with the fresh catalyst by XPS, FTIR, XRD and TEM and tested the UV tracking for Au_{25} NC (Figure S10-12). These characterizations showed that all parameters remained unchanged before and after the reaction, including the electronic structure and size of the embedded Au_{25} NC. At the same time, the mapping showed that the distribution of Au, S, Zn, Co and N of the recycled catalyst was the same as that of the fresh catalyst, indicating that ZIF-8@Au_{25}@ZIF-67[12] maintains high stability during the reaction.

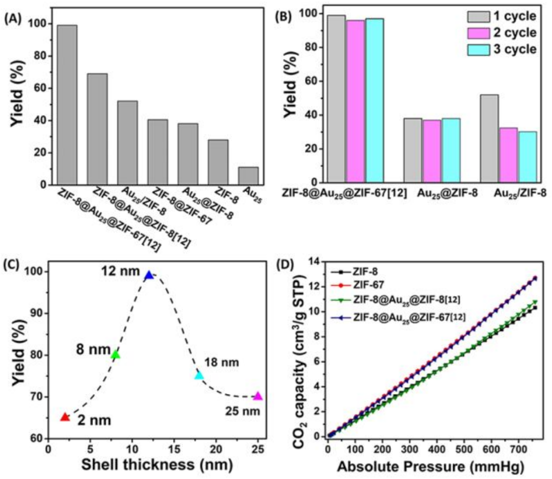

Figure 3. (A) Catalytic activity of various catalysts for the carboxylation of phenylacetylene. Reaction conditions: catalyst (1.12×10^{-4} mmol of Au_{25}), alkyne (0.5 mmol), Cs_2CO_3 (0.24 mmol), CO_2 (1.0 bar), 50 °C, 12 h. (B) Column diagram of three different catalysts. (C) Broken line diagram of catalytic performance of ZIF-8@Au_{25}@ZIF-67 with various shell thickness. (D) TPD-CO_2 by various catalysts.

Based on the stability of ZIF-8@Au_{25}@ZIF-67[12], we explored its tolerance to different functional groups (Table S3). Under optimal conditions, ZIF-8@Au_{25}@ZIF-67[12] exhibits good to excellent activity (83~99%) for carboxylation of substituted-phenylacetylene regardless of the electron-releasing or electron-withdrawing nature of the attached group. Besides, 2-ethylpyridine acetylene, propargylamine, cyclopropyl acetylene and trimethylsilylacetylene were also probed with ZIF-8@Au_{25}@ZIF-67[12] providing yields of 89.4%, 82.9%, 84.4% and 88.8%, respectively. Generally speaking, ZIF-8@Au_{25}@ZIF-67[12] was an excellent catalyst for the carboxylation reaction. Based on the experimental data and literature reports, a carboxylation mechanism is proposed in Figure 4. First, phenylene is deprotonated forming intermediate **II** under the combined action of Cs_2CO_3 and Au_{25} (confirmed by IR, Raman and NMR, see Figure S13-14), which is consistent with previous reports.[14] Then CO_2 is captured (confirmed by TPD-CO_2) and activated by 2-MIem of the ZIF-67 shell to give intermediate **III**.[13,15] Next, activated CO_2 inserts into the C≡C---Au bond to form intermediate **IV**. Finally, the products are released with regeneration of catalyst **I**.

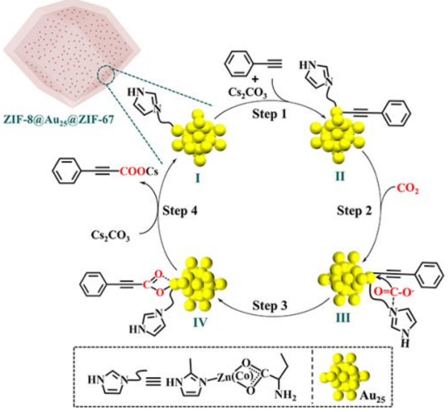

Figure 4. Proposed catalytic mechanism of the reaction between terminal alkynes and CO_2 over ZIF-8@Au_{25}@ZIF-67[tkn].

The 4-nitrophenol (4-NP) reduction is an excellent gauge of the performance of catalysts.[16] To verify the importance of the ultrathin shell, we further evaluated the catalytic properties of ZIF-8@Au_{25}@ZIF-67[12] for 4-NP reduction (Figure 5). Compared with Au_{25}@ZIF-8 and Au_{25}/ZIF-8, ZIF-8@Au_{25}@ZIF-67[12] exhibited superior catalytic performance. The TOF value is up to 588 min^{-1}, better than most reported catalysts in Table S4, due to the dual interface effect between Au_{25} NC and the MOF. In the meantime, the stability of ZIF-8@Au_{25}@ZIF-67[12] is particularly remarkable, maintaining excellent activity for at least 10 cycles. These results further demonstrate that the sandwich system not only facilitates stability but also accelerates activity.

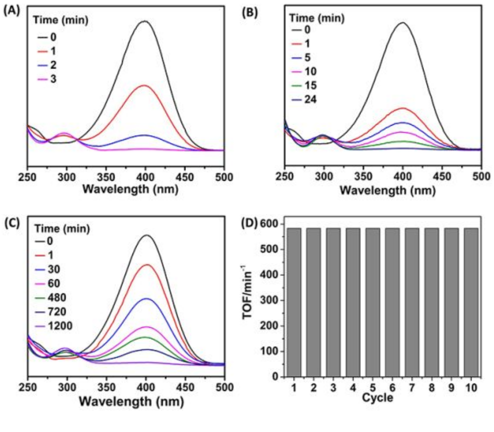

Figure 5. UV-Vis absorption spectra for 4-NP reduction by A) ZIF-8@Au_{25}@ZIF-67[12]; B) Au_{25}/ZIF-8. C) Au_{25}@ZIF-8. D) TOFs of recycled ZIF-8@Au_{25}@ZIF-67[12].

In summary, we have developed for the first time a coordination-assisted self-assembly method to control the fabrication of sandwiches ZIF-8@Au_{25}@ZIF-8[tkn] and ZIF-8@Au_{25}@ZIF-67[tkn]. These well-defined composites feature simultaneously improved activity and stability for terminal alkyne carboxylation using CO_2 and 4-NP hydrogenation. Interestingly, the catalytic performance of the sandwich system is easily optimized by precise adjustment of the shell thickness. Therefore, this work should stimulate the interest of nanochemists toward the design of well-defined sandwich composites MOF@APNC@MOF with perfect properties and open up new horizons for nanomaterial studies.

ASSOCIATED CONTENT

Supporting Information

The Supporting Information is available free of charge on the ACS Publications website at DOI:
Experimental procedures, crystallographic data, TEM, BET, UV-vis., Raman, XPS, XRD, IR, and absorption spectra (PDF)

AUTHOR INFORMATION

Corresponding Authors

shenght@ahu.edu.cn; didier.astruc@u-bordeaux.fr
zmz@ahu.edu.cn

Notes

The authors declare no competing financial interests.

ACKNOWLEDGMENT

We acknowledge financial support by the National Natural Science Foundation of China ((21972001, 21871001), Anhui University, University of Bordeaux and CNRS.

REFERENCES

(1) (a) Ding, M.; Flaig, R. W.; Jiang, H.-L.; Yaghi, O. M. Carbon capture and conversion using metal-organic frameworks and MOF-based materials. *Chem. Soc. Rev.* **2019,** *48,* 2783-2828. (b) Wang, X.; Li, Z.; Qu, Y.; Yuan, T.; Wang, W.; Wu, Y.; Li, Y. Review of Metal Catalysts for Oxygen Reduction Reaction: From Nanoscale Engineering to Atomic Design. *Chem,* **2019,** *5,* 1486–1511. (c) Liu, L.; Corma, A. Metal Catalysts for Heterogeneous Catalysis: From Single Atoms to Nanoclusters and Nanoparticles. *Chem. Rev.* **2018,** *118,* 4981-5079. (d) Deng, D.; Novoselov, K. S.; Fu, Q.; Zheng, N.; Tian, Z.; Bao, X.; Catalysis with two-dimensional materials and their heterostructures. *Nat. Nanotech.* **2016,** *11,* 218-230. (e) Samantaray, M. K.; D'Elia, V.; Pump, E.; Falivene, L.; Harb, M.; Chikh, S. O.; Cavallo, L.; Basset, J.-M. The Comparison between Single Atom Catalysis and Surface Organometallic Catalysis. *Chem. Rev.* **2020**, *120*. 734-813.

(2) (a) Xu, L.; Liang, H.-W.; Yang, Y.; Yu S.-H. Stability and Reactivity: Positive and Negative Aspects for Nanoparticle Processing. *Chem. Rev.* **2018,** *118,* 3209-3250. (b) Yang, F.; Abadia, M.; Chen, C, Wang, W.; Li, L.; Zhang, L.; Rogero, C.; Chuvilin, A.; Knez, M. Design of active and stable oxygen reduction reaction catalysts by embedding Co_xO_y nanoparticles into nitrogen-doped carbon. *Nano Research,* **2017,** *10,* 97-107.

(3) (a) Molnár, Á.; Papp, A. Catalyst recycling-A survey of recent progress and current status. *Coord. Chem. Rev.* **2017,** *349,* 1-65. (b) Wang, W.; Cui, L.; Sun, P.; Shi, L.; Yue, C.; Li, F. Reusable N-Heterocyclic Carbene Complex Catalysts and Beyond: A Perspective on Recycling Strategies. *Chem. Rev.* **2018,** *118,* 9843-9929. (c) Sudarsanam, P.; Peeters, E.; Makshina, E. V.; Parvulescu,V. I.; Sels, B. F. Advances in porous and nanoscale catalysts for viable biomass conversion. *Chem. Soc. Rev.* **2019,** *48,* 2366-2421.

(4) (a) Yang, X.; Sun, J.-K.; Kitta, M.; Pag, H.; Xu, Q. Encapsulating highly catalytically active metal nanoclusters inside porous organic cages. *Nat. Catal.* **2018,** *1,* 214-220. (b) Ernst, J. B.; Muratsugu, S.; Wang, F.; Tada, M.; Glorius, F. Tunable Heterogeneous Catalysis: N−Heterocyclic Carbenes as Ligands for Supported Heterogeneous Ru/K-Al_2O_3 Catalysts to Tune Reactivity and Selectivity. *J. Am. Chem. Soc.* **2016,** *138,* 10718-10721. (c) Du, Y.; Sheng, H.; Astruc, D.; Zhu, M. Atomically Precise Noble Metal Nanoclusters as Efficient Catalysts: A Bridge between Structure and Properties. *Chem. Rev.* **2019,** *119,* 526-622.

(5) (a) Yang, Q.; Xu, Q.; Jiang, H.-L. Metal-organic frameworks meet metal nanoparticles: synergistic effect for enhanced catalysis. *Chem. Soc. Rev.* **2017,** *46,* 4774-4808. (b) Wang, S.; McGuirk, C. M.; d'Aquino, A.; Mason, J. A.; Mirkin, C. A. Metal–Organic Framework Nanoparticles. *Adv. Mater.* **2018,** *30,* 1800202. (c) Wang, N.; Sun, Q.; Yu. J. Ultrasmall Metal Nanoparticles Confined within Crystalline Nanoporous Materials: A Fascinating Class of Nanocatalysts. *Adv. Mater.* **2019,** *31,* 1803966. (d) Q. Wang; D. Astruc. State of the Art and Prospects in Metal–Organic Framework (MOF)-Based and MOF-Derived Nanocatalysis. *Chem. Rev.* **2020,** *120,* 1438-1511. (e) Wang, C.; Tuminetti, J.; Wang, Z.; Zhang, C.; Ciganda, R.; Moya, S.; Ruiz, J.; Astruc, D. Hydrolysis of Ammonia-Borane over Ni/ZIF-8 Nanocatalyst: High Efficiency, Mechanism, and Controlled Hydrogen Release. *J. Am. Chem. Soc.* **2017,** *139,* 11610–11615.

(6) (a) Lu, G.; Li, S.; Guo, Z.; Farha, O. K.; Hauser, B. G.; Qi, X.; Wang, Y.; Wang, X.; Han, S.; Liu, X.; DuChene, J. S.; Zhang, H.; Zhang, Q.; Chen, X.; Loo, S. C. J.; Wei, W. D.; Yang, Y.; Hupp J. T.; Huo, F. Imparting functionality to a metal–organic framework material by controlled nanoparticle encapsulation. *Nat. Chem.* **2012,** *4,* 310-316. (b) Yang, Q.; Liu, W.; Wang, B.; Zhang, W.; Zeng, X.; Zhang, C.; Qin, Y.; Sun, X.; Wu, T.; Liu, J.; Huo, F.; Lu, J. Regulating the spatial distribution of metal nanoparticles within metal-organic frameworks to enhance catalytic efficiency. *Nat. Commun.* **2017,** *8,* 14429. (c) Wan, M.; Zhang, X.; Li, M.; Chen, B.; Yin, J.; Jin, H.; Lin, L.; Chen, C.; Zhang, N. Hollow Pd/MOF Nanosphere with Double Shells as Multifunctional Catalyst for Hydrogenation Reaction. *Small* **2017,** *13,* 1701395. (d) Chen, L.; Chen, H.; Luque, R.; Li, Y. Metalorganic framework encapsulated Pd nanoparticles: towards advanced heterogeneous catalysts. *Chem. Sci.* **2014,** *5,* 3708-3714.

(7) Zhao, M.; Yuan, K.; Wang, Y.; Li, G.; Guo, J.; Gu, L.; Hu, W.; Zhao, H.; Tang, Z. Metal–organic frameworks as selectivity regulators for hydrogenation reactions. *Nature* **2016,** *3,* 76-80.

(8) (a) Chakraborty, I.; Pradeep, T. Atomically Precise Clusters of Noble Metals: Emerging Link between Atoms and Nanoparticles. *Chem. Rev.* **2017,** *117,* 8208−8271. (b) Zeng, C.; Zhou, M.; Chen. Y.; Jin. R. Atomically Precise Colloidal Metal Nanoclusters and Nanoparticles: Fundamentals and Opportunities. *Chem. Rev.* **2016,** *116,* 18, 10346-10413. (c) Shen, H.; Deng, G.; Kaappa, S.; Tan, T.; Han, Y.; Malola, S.; Lin, S.; Teo, B., Häkkinen, H., Zheng, N.; Highly Robust but Surface-Active: N-Heterocyclic Carbene-Stabilized Au_{25} Nanocluster, *Angew. Chem. Int. Ed.* **2019,** *131,* 17895-17899.

(9) Yuan, X.; Zhang, B.; Luo, Z.; Yao, Q.; Leong, D. T.; Yan, N.; Xie, J. Balancing the Rate of Cluster Growth and Etching for Gram-Scale Synthesis of Thiolate-Protected Au_{25} Nanoclusters with Atomic Precision. *Angew. Chem. Int. Ed.* **2014,** *126,* 4711-4715

(10) Yu, S.; Li, S.; Huang, S.; Zeng, Z.; Cui, S.; Liu, Y. Covalently bonded zeolitic imidazolate frameworks and polymers with enhanced compatibility in thin film nanocomposite membranes for gas separation. *J. Membrane Sci.* **2017,** *540,*155-164.

(11) Bachari, E.M.; Baud, G.; Jacquet M. Structural and optical properties of sputtered ZnO films. *Thin Solid Films* **1999,** *348,* 165-172.

(12) Luo, Y.; Fan, S.; Yu, W.; Wu, Z.; Cullen, D. A.; Liang, C.; Shi, J.; Su, C. Fabrication of $Au_{25}(SG)_{18}$-ZIF-8 Nanocomposites: A Facile Strategy to Position $Au_{25}(SG)_{18}$ Nanoclusters Inside and Outside ZIF-8. *Adv. Mater.* **2018,** *30,* 1704576.

(13) Zanon, A.; Chaemchuen, S.; Mousavi, B.; Verpoort, F. Bibimaryam Mousavia, Francis Verpoort, Zn-doped ZIF-67 as catalyst for the CO_2 fixation into cyclic carbonates. *J. CO_2 Util.* **2017,** *20,* 282-291.

(14) (a) Maity, P.; Takano, Wakabayashi, T.; Tsukuda, T. Binding Motif of Terminal Alkynes on Gold Clusters. *J. Am. Chem. Soc.* **2013,** *135,* 9450-9457. (b) Li, G.; Jin, R. A Unique Activation Pathway for Terminal Alkynes. *J. Am. Chem. Soc.* **2014,** *136,* 11347-11354.

(15) (a) Zeng, S.; Zhang, X.; Bai, L.; Zhang, X.; Wang, H.; Wang, J.; Bao, D.; Li, M.; Liu, X.; Zhang, S. Ionic-Liquid-Based CO_2 Capture Systems: Structure. *Chem. Rev.* **2017,** *117,* 9625-9673. (b) Hu, Y.; Liu, Z.; Xu, J.; Huang, Y.; Song, Y. Evidence of Pressure Enhanced CO_2 Storage in ZIF-8 Probed by FTIR Spectroscopy. *J. Am. Chem. Soc.* **2013,** *135,* 9287-9290.

(16) (a) Herves, P.; Perez-Lorenzo, M.; Liz-Marzan, LM.; Dzubiella, J.; Lu, Y.; Ballauff, M. Catalysis by metallic nanoparticles in aqueous solution: model reactions. *Chem. Soc. Rev.* **2012,** *41,* 5577-5587. (b) Aditya, T.; Pal, A.; Pal, T. Nitroarene reduction: a trusted model reaction to test nanoparticle catalysts. *Chem. Commun.* **2015,** *51,* 9410-9431. (c) Zhao, P.; Feng, X.; Huang, D.; Yang, G.; Astruc, D. Basic concepts and recent advances in nitrophenol reduction by gold- and other transition metal nanoparticles. *Coord. Chem. Rev.* **2015,** *287,* 114-136.

TOC graphic：

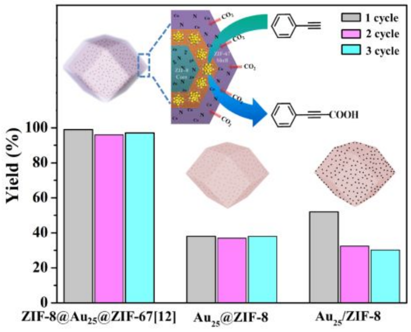
1 cycle
2 cycle
3 cycle
COOH
Yield (%)
0
20
40
60
80
100
ZIF-8@Au$_{25}$@ZIF-67[12]
Au$_{25}$@ZIF-8
Au$_{25}$/ZIF-8